Paul R. Moran, Ph.D.
Richard A. Moran, B.S.[2]
Nolan Karstaedt, M.B., B.Ch.

Verification and Evaluation of Internal Flow and Motion

True Magnetic Resonance Imaging by the Phase Gradient Modulation Method[1]

We report qualitative and quantitative evaluation and verification studies of the bipolar phase gradient modulation method for true MR imaging of internal flow and motion velocities. Velocity encoding modulations provide speed-of-motion and direction-sensitive images using special phase-sensitive reconstructions. True motion MR imaging does not depend upon subject parameters, T1 or T2, nor upon selective active-volume time-of-flight calculations, nor is it limited strictly to fluid-flow velocities. Conventional MR sequences often induce strong *accidental* phase gradient modulations that can cause severe artifacts in conventional MR scans and limit the useful sensitivities of true motion MR. Multiple steps of velocity encoding allow resolution of separate elements of the *velocity spectrum*, and enable suppression of all such phase-artifact difficulties. Some view-to-view phase inconsistencies are intrinsic to the subject being scanned, *e.g.*, strong motion variations during the heart cycle; limitations due to such effects require external modifications in the scanning, such as cardiac gating. Since conventional density information remains in the data, independent of velocity encoding modulations, we suggest a multiple encoding sequence and saving the MR raw data. These evaluations and verifications demonstrate exciting potential in clinical application for the phase gradient modulation method of true flow and motion MR imaging.

Index terms: Flow dynamics • Magnetic resonance, technology • Magnetic resonance

Radiology 1985; 154: 433-441

Two decades before magnetic resonance (MR) medical imaging became feasible, studies showed that MR signals respond to motions of molecules and, in particular, to flow in a liquid sample. Singer reported a non-imaging MR observation of blood flow (1). More recently, Battocletti, *et al.* (2) extensively reviewed the long history, theory, design, and applications of non-imaging MR blood-flow measurements. Consequently, knowledgable investigators recognized immediately the importance of *flow imaging* when human MR imaging proved possible. Unfortunately, it has been far easier to claim flow imaging in principle than to demonstrate a real specific and reliable method in practice for combining MR-flow information with MR-imaging capability.

Strong qualitative image disturbances often appear in conventional MR images and are attributed to flow or other motion. Such effects vary drastically, however, with changes in scanner sequence parameters (3). Moreover, recent studies show that completely different qualities for these flow-related perturbations of conventional MR images occur with scanners of different manufacturers and even change with the details chosen for the particular image reconstruction algorithm (4, 5). These behaviors result in great confusion in nomenclature, meaning, and concept in this area of MR research and applications.

A first category of flow-related phenomena, *time-of-flight effects*, was used to explain almost all of the previously observed flow-disturbances in conventional MR images (6, 3). The principle underlying all time-of-flight effects is to create a well-defined active volume of MR excitation at one position and instant of time and then reexamine at a later instant of time. One example is the flow of *fresh spins* into a previously excited and *saturated* section. Preliminary success in quantitating such effects using multiple MR imaging scans to evaluate blood flow in humans has been reported (7).

A second category of MR motion effects is phase shifts. When precessing magnetic moments move in a magnetic field gradient, then they exhibit a frequency shift related to their velocity along the gradient direction. This phenomenon is analogous to Doppler shift in ultrasound studies. The frequency shift multiplied by the time duration of its occurence gives the accumulated number of precession cycles gained or lost with respect to unshifted magnetic moments; this relative accumulation is called the phase shift. However, the whole principle of MR imaging, for non-moving magnetization, depends upon large modulations of magnetic field gradients over hundreds of cycles of variation. This produces large frequency and phase modulations to encode the MR signals for their average *positions* (not velocities). The encoded data later reconstruct into the desired spatial image. Consequently, small velocity-dependent phase shifts of non-specific character become completely entangled and lost in the overwhelming influences of the MR imaging process itself.

In 1982 a theory and proposal for a special phase-gradient-modu-

[1] From the Department of Radiology, Bowman Gray School of Medicine, Winston Salem, North Carolina.
Received Nov. 22, 1983; accepted and revison requested Jan. 10, 1984; revision received Sep. 19.
[2] Present address: General Electric Medical Systems, NMR Division, P.O. Box 414, Milwaukee, Wisconsin.

cp

Figure 1

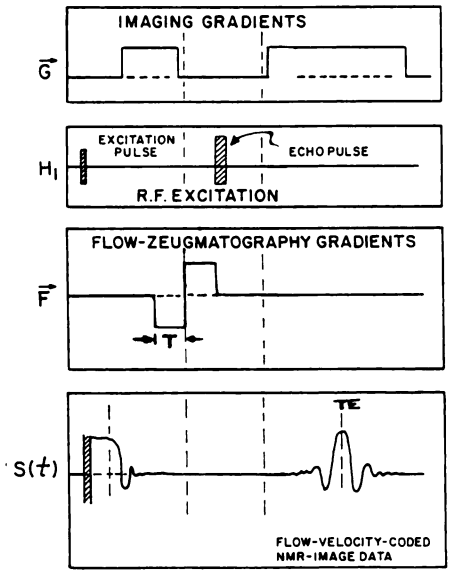

Schematic illustration of the spin echo parent image MR sequence used in these studies, together with the special phase gradient modulation (F gradients) for velocity encoding.

lation technique in MR imaging was developed (8). The technique produces a specific and controlled velocity-dependent phase modulation; it can be interlaced into any already existing MR imaging sequence without interference, and its velocity-encoding is disentangled and separable from the position-encoding imaging modulations. The phase-modulation method encodes directly the components of velocity-of-motion as true subject variables of the magnetization to be imaged, just as the conventional imaging modulations encode the spatial positions of the magnetization as subject variables.

It is helpful to stress certain aspects of the phase-modulation method in MR imaging of motion and flow. When a true and direct velocity phase-modulation of the data is achieved, then:

- One obtains a completely different kind of imaging possibility from that of the flow-related disturbances visualized previously in conventional MR images.

- There is no need to excite selectively in some way an active volume for observation of time-of-flight changes. This technique relies upon phase-modulation of existing magnetizations rather than upon inducing scan-to-scan magnitude variations (For example, velocity-encoding may interlace directly into three dimensional volumetric MR imaging modes.)

- Velocities of motion are intrinsically coded and intrinsically imagable directly. An ordinary reconstruction of magnetization magnitude subsequently produces an ordinary magnitude MR image, while a modified reconstruction of the same data yields a second image reflecting (in a number of flexible display choices) the velocity-density of motion.

- When a distribution of different spatially unresolvable velocities occurs in a single imaged voxel, then a series of velocity-modulations allows imaging of the velocity spectrum. This occurs in exactly the same way as chemical shift spectrum imaging yields separate images of nuclear moments situated in different chemical molecular-sites.

- In a specific situation, whatever velocity component is deemed of clinical interest can be chosen specifically for imaging. Motions perpendicular to the image plane or motions with any specified component within the image plane can be phase-modulation sensitized, encoded, and imaged.

To stress these fundamental differences from other flow-related effects in MR images, we refer to the phase-modulation methods as *true flow imaging*, or generally as *true motion imaging*. This emphasizes that the motion quantity (velocity) truly has been encoded as an MR imaging variable and can directly be reconstructed as such. We do not mean to imply, however, that other approaches to flow estimation and evaluation in MR imaging necessarily give untrue results.

Subsequent to the original theory and proposal many investigators (including those from this laboratory) recently have given some experimental verifications and practical applications (8, 5, 6, 9–11). Eight additional confirmations more recently were presented in scientific sessions or commercial exhibits (12–19). The purpose of this paper, however, is to present some simple rudimentary phantom studies (and a preliminary example of human studies) to demonstrate the fundamental meaning and impact of true motion images. We also wish to show empirical validation of the quantitative essentials of the basic theory, and to evaluate the applicability and current limitations of the phase-modulation method for true motion MR imaging.

METHOD

Pulse Sequence. Figure 1 illustrates a review of the pulse sequence for which a complete technical description occurs elsewhere (5, 10, 20). The gradients, radio frequency (*rf*) excitations, and data acquisition intervals depicted are for one of the many cyclic views of an MRI-scan. The example shown is a spin-echo sequence, and it is the sequence essentially as used in the scans presented later. The bipolar form modulation pulse labeled "flow-zeugmatography gradients" is the added phase-gradient-modulation element, which provides specific velocity encoding. Consider first the situation where we omit the special F-modulation entirely; then the sequence is just a conventional MR spin-echo cycle.

In the conventional cycle, an rf excitation 90° pulse occurs with simultaneous section selection imaging gradients (shown as the broken lines in the G-gradient box of Fig. 1). The section selection gradient is perpendicular to the plane of the section; this process requires a subsequent rephasing interval shown as the negative broken line. Next, one activates imaging gradients in the image plane, as indicated by the solid line. They produce an encoding step in one direction and a prereadout modulation in the remaining direction. The demodulated MR signal data are from a pair of phase-coherent electronic demodulators; two channels of output signals result (in the figure, S(t) illustrates only one of them). A reference in-phase from the rf excitation source yields one channel, and a reference in quadrature (90° phase shfit) from the rf excitation yields the second. This is standard instrumentation for all modern MR scanners. A free induction decay (FID) waveform is depicted by S(t) after excitation (the far left in the figure).

For practical reasons, modern MR imagers do not use the direct FID signals, but acquire image reconstruction data from echo FID waveforms, which is illustrated by the pattern occurring at *TE* (time-of-echo) in the figure. These echo data occur as a result of the 180° echo rf-pulse excitation indicated, together with reapplication of the readout gradient (illustrated as the final solid line modulation in the G-gradient box). As described so far, the MR data occurring around TE correspond to conventional MR data.

For specific velocity sensitization, the bipolar (*i.e.*, having equal and opposite portions) F-gradient form is added to the sequence. This phase gradient modulation can be chosen in any spatial direction by activating appropriately a combination of the three perpendicular field-gradient coils. The velocity sensitizing modulation is special because of its temporal form and position preceeding the readout, rather than because it is necessarily generated by different physical coils from those used (also) for conventional imaging gradients. The result is that any magnetization, excited at any spatial position, receives an added discrete phase modulation. This is proportional to the velocity component along the F direction. The phase modulation angle, in fractions of a full 360° of precession, is given by

$$\langle \text{phase angle} \rangle = [\text{gamma} \times F] \times T^2 \times V \quad \text{(Equation 1)}$$

where [gamma × F] is the strength of the bipolar velocity sensitizing modulation in hertz per centimenter, T is the biopolar modulation time in seconds (see Fig. 1), and V is the velocity (centimeters per second) along the direction of F, at the position in question. When these steps occur, the MR data carry added specific velocity phase encodings for each pixel in the image.

Image Reconstruction. From the two quadrature data channels (described above), one always can reconstruct two independent images. The first is the ordinary (so-called *real*) image corresponding to the image of in-phase magnetization excited. The second image is the quadrature (so-called *imaginary*) image; it displays the quadrature phase magnetization excited. One normally expects the second image to be a completely null-image (zero everywhere except for noise). This is because there would be no quadrature magnetization excited normally (apart from phase error artifacts or special added modulations we attempt to exploit for motion-imaging). Consequently, conventional MR imaging either never calculates the quadrature image at all or else (should spurious phase-errors occur) forms the square-root of the sum-of-squares of the two images, pixel by pixel, to produce a resulting final phase insensitive magnitude (or modulus) image.

Using a conventional phase insensitive reconstruction guarantees that any velocity phase coding will be discarded, and a conventional image will result. To reveal the velocity effects, the reconstructions must extend to the *velocity dimension*, and many clever phase sensitive algorithms for accomplishing this have been discussed recently (5, 9–11, 16).

We can illustrate all of the essential principles, demonstrate prototypes of practical scans, systematically verify the crucial theoretical predictions, and show the evaluations and limitations of the method by employing a very crude reconstruction alternative. In pre-processing, we simply treat the raw data by assuming mathematically that there are no added phase shifts; this provides an overall average phase centering against which the velocity dependent phase modulations will add local phase variations. In this case, the predicted real image (which we can reconstruct and display separately) will be modified spatially by multiplication by cosine ⟨phase angle⟩. The most sensitive motion image will be the quadrature phase image (which we can reconstruct and display separately), and it will be essentially a conventional *density* image modified spatially by multiplication by sine ⟨phase angle⟩. If the motion along F has zero velocity, the ⟨phase angle⟩ is zero from Equation 1; the in-phase real image will just be a standard image since cosine ⟨0⟩ is unity, and the quadrature image will be a null-zero image since sine ⟨0⟩ is zero.

We earlier found phase artifacts in scans of non-moving subjects (5). To compensate crudely for these in the current simple implementation, we can perform a separate scan having no velocity modulations, and then subtract the two image versions. Or we can take a positive (forward modulated) scan and subtract a negative encoded (backward modulated) scan, or use some combination. Common phase errors tend to cancel. This may work for phantoms, but humans are significantly less controllable; for example, several millimeter long term displacements between scans, typical of living subjects, defeats such simplicities. One needs to vary modulation parameters on sequential cycles (and maintain appropriate bookkeeping of the raw data); then misregistrations from long term patient motion can be largely eliminated. Investigators from manufacturer's research laboratories, where access to developmental level software is supported, have demonstrated the success of such modifications (11, 13, 15). We have only clinical scan version of software available to us, however, and cannot yet implement sophisticated improvements in human studies in a practical way.

Related Observations. At least two equivalent methods to achieve the same physical phase-gradient bipolar-modulation for motion-encoding (shown in Fig. 1 in the flow-zeugmatography gradients box) have been detailed (8). The earliest trials demonstrated both successfully (4, 5). The first approach is an electronic reversal of the magnetic field gradient modulation in the successive halves as is implied by the sketch of the F-gradient activation in Figure 1. The second approach is a positive field gradient first half, followed by a 180° rf pulse (which inverts the phase gradient of the magnetization), followed by another positive field gradient second half.

An important consequence is observed by studying the conventional imaging gradients (the G-gradient box) in Figure 1. The 90° section selection process inherently involves a field gradient reversal (perpendicular to the section), and the solid line readout gradients involve a 180° rf pulse reversal. Moreover, when the conventional echo pulse process also is a section selective type (necessary for multi-section modes), then additional (10) bipolar phase-gradient-modulations occur.

This means that some conventional-sequences *accidentally* induce the kind of velocity-encoding modulations we have discussed; the theory predicts that an appropriate phase sensitive reconstruction of those data will, therefore, yield motion images. The interlaced phase gradient modulation already exists and can be used, although its properties may not be entirely appropriate to the controlled sensitizations desired (a human study example is shown later). Perhaps more important, when these accidental phase gradient modulations remain uncompensated and coexist in a scan where further controlled modulations are desired also, then one can obtain inconsistent phase modulation from the combination. The result can be motion-sensitive images dominated by velocity dependent (especially motion components perpendicular to the desired direction) artifacts and spurious structures.

A second important observation is that an MR imaging scan requires many sequential views, each carrying a different *spatial* field gradient encoding to extract the two dimensional static spatial-position information. The velocity sensitizing phase modulation, on the other hand, must remain constant from view to view; if the flow or motion velocities vary significantly from view to view during the scan, then the phase modulations will be inconsistent among the views. The consequence, predicted by the theory, can be an image where rapidly and erratically moving materials have their image intensity removed from their true position by the reconstruction algorithm. In this case, the affected image intensities reappear as a quasi-random *splatter* (resembling random noise) dispersed unpredictably over the entire field of view.

Finally, we re-emphasize the observation that the phase modulation techniques for true motion-imaging, as well as time-of-flight approaches, respond to the velocity of motion of the molecules bearing the magnetization excited in the MR process. The class of such motions in living subjects comprises more than simply physical fluid flow, *e.g.*, blood in vessels; any tissue motion can, in principle, be imaged. Initial confirmation in the application to imaging heart muscle motion appeared in preliminary descriptions elsewhere, and one example extended from those studies is discussed later in this article (5, 10).

MATERIALS

Phantom. A polyethylene square-bottle, 10 × 10 cm in cross section and 18 cm in height, is the non-moving-liquid container of our simple flow phantom. Four holes at the same height, a pair in opposite vertical faces, allow insertion of a horizontally oriented U-tube of nominal 1 cm inside diameter (ID) surgical Tygon tubing to hold flowing liquid. The U-bend, which gives a semicircular flow pattern, extends 15 cm into the air beyond the back surface. Common silicone caulking provides a non-magnetic seal between the bottle and the flow tube. Thus in the horizontal plane, which we can image with a coronal section, we obtain a flowing liquid contrast against a non-flowing liquid, a flowing liquid contrast against air (no MR signals), and a non-flowing liquid contrast against air. The U-tube form (horizontal plane in the laboratory) corresponds to the form of a coronal section in a patient and the tube cross sections to the transverse section.

Five centimeters under the U-tube described above, we inserted a second similar U-tube using 1.3 cm nominal ID Tygon tubing. This tube contained only air (no MR active material); by performing transverse scanning we then had the upper U-tube cross-sections with into- and out-of-section flow, displayed simultaneously with two corresponding air-filled cross sections below. A transverse MR scan (Fig. 2) thus displays the same contrasting sets (flowing-liquid in two directions, non-flowing liquid, and air-filled regions) as described for the coronal (horizontal-plane) scan.

Distilled water, doped with paramagnetic manganese acetate to several micro-molar solute, is both the non-moving and the flowing liquid; adjustment by dilution gives the same T1 values (about 500 msec) as human blood at our operating frequency of

Figure 2

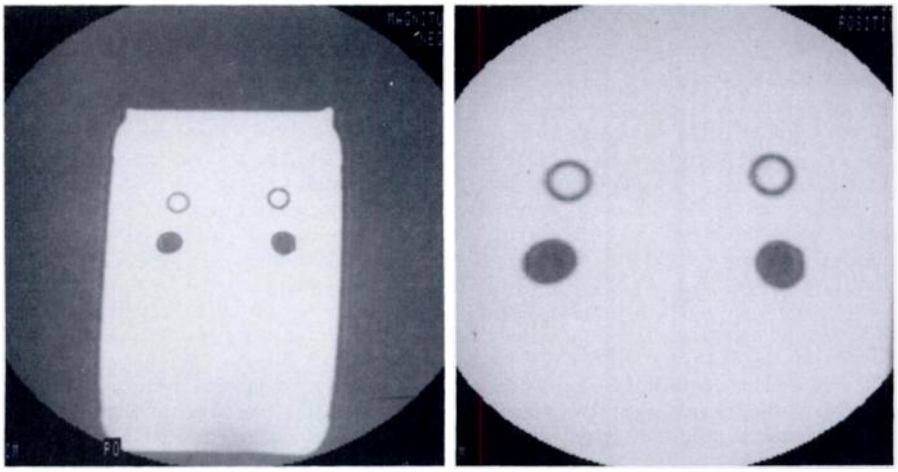

a. b.

Transverse images of the flow phantom showing conventional magnitude reconstruction images.
a. A negative sense velocity encoding.
b. A 2 × magnification of a positive sense encoding.

6.25 MHz (hydrogen Larmor frequency at 0.15 T). Tubing extensions connect the U-tube with a large carboy reservoir for the flowing liquid source, and to an open out-flow reservoir. Changing the difference between the source reservoir water-height and the out-flow exit gives simple and reliable control of gravity-pressure and thereby the flow rate in the tubing. Once established, the flow remains nearly constant throughout a scan because the source reservoir is large compared with the flow volumes typically occurring. Timing the out-flow into a large graduated cylinder gives direct measure of the volume-flow rate for that scan; dividing the volume rate by the known U-tube cross-sectional area gives the average flow speed along the tube.

With this simple arrangement, we could achieve and maintain reliably average flow velocities from a few tenths of a centimeter per second up to 30 centimeters per second (at the highest rates, nearly continuous manual transfer from out-flow reservior to source-reservoir containers was necessary to maintain constant waterhead pressure).

Scanner. The MR scans were obtained using the head-coil and head-scanning modes of a Picker International 1000, an MR resistive magnet imager operating at 0.15 T. Software in the standard clinical scan program allows additions to the sequence of various phase gradient modulation forms, separate access to the in phase (real), to the quadrature phase (imaginary), and to the magnitude image reconstructions, and provides off-line utilities for subtractions and additions of different scan data.

The parent sequence we chose for modification is a standard SE 20 (the 180° rf echo-pulse in Fig. 1 occurs 20 msec after the initial 90° rf excitation) using two dimensional Fourier transform image encoding. The section profile is relatively sharply edged with a full-width of 10 mm. The single-section mode echo pulses were short, broadband, non-selective excitations; only the initial 90° excitations are selective in single-section mode. Non-selective pulses tend to saturate the entire subject's magnetization uniformly and thereby minimize *fresh-spin* inflow or other time-of-flight effects into these phase-modulation studies. Cycle repetition times typically were 500 msec.

For the several purposes of this evaluation, we chose different parameters for the bipolar phase gradient modulation (the F-modulation form in Fig. 1).

- To demonstrate true flow imaging for motion perpendicular to the section we used the transverse scan shown in Figure 2. Here, we employ the direct field gradient reversal implementation to achieve velocity phase encoding, and use pulse times and gradient strengths to give (according to our scanner's calibration factors) numerical values for Equation 1 of

  ⟨phase angle⟩
  = [0.025 (seconds per centimeter)] × V
  (Equation 2)

  When V is the flow velocity component perpendicular to the image plane (in centimeters per second), then Equation 2 gives the velocity phase modulation of the data in fractions of a full cycle of magnetization precession.

- For motion imaging in the plane of the section, we used coronal scans. In this case, we chose to use the rf-echo implementation for achieving the bipolar phase gradient modulation. We used these scans also to demonstrate a stronger velocity sensitization by choosing the gradients and times to provide numerical factors in Equation 1 of

  ⟨phase angle⟩
  = [0.2 (seconds per centimeter)] × V
  (Equation 3)

  The sensitized component, V, is in the direction that, as veiwed in the displayed image, appears *vertical* (axial flow in the supine patient) in this case. For a human study, we used the in-the-plane encoding as above, but changed it to exemplify horizontally directed motion in a transverse section (and with a velocity-sensitivity two thirds that given in Equation 3).

It is scanner gradient calibrations (not flow phantom calibrations) that give the numerical sensitivities predicted in Equations 2 and 3. We will compare these against the quantitative results of the experiments described later. For example, when the ⟨phase angle⟩ of Equations 1, 2, or 3 attains a value of one quarter cycle, then the true velocity image values should rise from zero to a maximum value just equal to that observed in a conventional image, for a single scan. Using the positive-minus-negative scans technique to compensate unrelated phase-artifact, then true motion image values should be twice those in a conventional single-scan reconstruction.

RESULTS

Transverse motion. The scans of Figure 2 show a conventional magnitude reconstruction in transverse section. The flow in the upper U-tube set enters (velocity away from the viewer) on the right tube of the display (patient's left side) and exits (velocity toward the viewer) on the left tube of the display. The plastic tubing walls give a dark cross section annulus, and the lower U-tube set (filled with air) demonstrates conventional MR air-to-water contrast. Figure 2a shows normal field-of-view with a negative sense modulation (the sensitizing gradient first goes negative and then positive); Figure 2b is a 2 × magnification (for later reference) and shows a positive sense modulation. The flow speed is an average 5 cm/sec, but the images displayed are indistinguishable from each other, and from unmodulated scans. A conventional phase insensitive magnitude of magnetization reconstruction gives, as predicted, a conventional MR image.

Figure 3a shows the phase-sensitive reconstruction from the same raw data used in Figure 2b. We predict it to be the magnetization density multiplied everywhere by *sine ⟨phase angle⟩*. As predicted, the flow velocity away from the viewer has strong positive image values (brighter in display), since sine ⟨phase angle⟩ is positive. The return flow toward the viewer shows opposite negative value (blacker in the display) contrast, since the sine ⟨phase angle⟩ is negative. Motionless material in the phantom body, however, is not uniformly at zero value as would be expected in the ideal true motion image. This is some phase artifact of unknown

origins; the scan shown in Figure 3b illustrates the same phase artifact even when the flow is turned off. By using negative sense phase modulation, the scan in Figure 4a results. It shows the reversed sense of flow contrast predicted with respect to the positive modulation in Figure 3, and also exhibits similar phase error artifacts. By subtracting the image data of the negative modulation scan from that of the positive modulation scan, the phase error artifacts tend to cancel. This is shown in Figure 4b where essentially only the true flow image appears. Velocities away from the viewer are imaged as positive values, those toward the viewer are negative values, and non-moving material images as null-zero everywhere in Figure 4b; note that the lower air-filled tubes become completely non-contrasting, as predicted, against non-flowing liquid in the phantom body.

Figure 5 demonstrates flow profiles and quantitative verification of some theoretical predictions. Figures 5a is the 2 × magnification of the conventional image of Figure 2b, but at different display settings so that a software profile line and plot of image values across that line can be seen. Within the flow tube cross sections, the flowing liquid MR values have a magnitude of approximately 80 units (these are arbitrarily scaled values, but maintain the same scaling for a given constant setting of the instrument's receiver gain).

Figure 5b is a 2 × magnification of that shown in Figure 4b imaging the positive-minus-negative modulated scans data. Note the disappearance of non-moving liquid (the air-filled cross sections vanish into background). The MR value trace across the flowing sections shows a parabola-like shape reflecting the velocity profile across the tube. We adjusted the average flow velocity upward until the maximum central value stopped increasing and began slightly to decrease (where sine ⟨phase angle⟩ decreases because ⟨phase angle⟩ increases beyond one quarter cycle). Then we slightly reduced the flow to give nearly maximum excursion (this is where the maximum velocity gives approximately a quarter cycle phase shift) for the scan of Figure 5b. The measured average flow velocity under these conditions was 5 cm/sec. The MR values in the true flow image cross sections reach a peak of about 160 MR units, positive for in-flow and negative for out-flow. This verifies the theoretical prediction that the simple flow image maximizes at the conventional image values. Here, the compensated modulation images subtract two op-

Figure 3

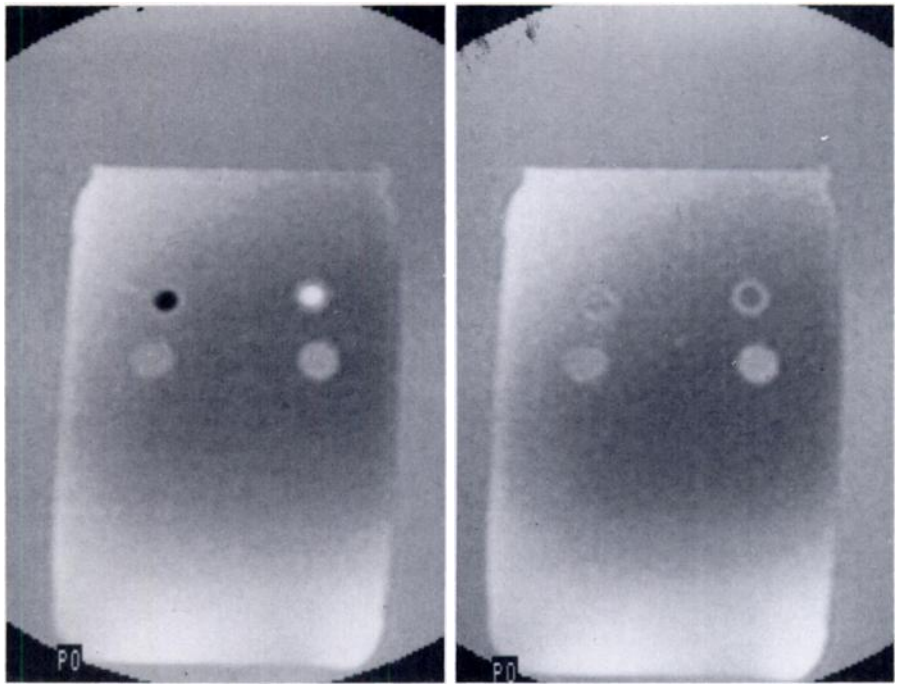

a. b.

a. Reconstruction of the quadrature image (from data of Fig. 2b) shows into-the-section and out-of-the-section flow contrasts.
b. Phase errors unrelated to motion give data artifacts and residual contrast patterns in the nonflow image.

Figure 4

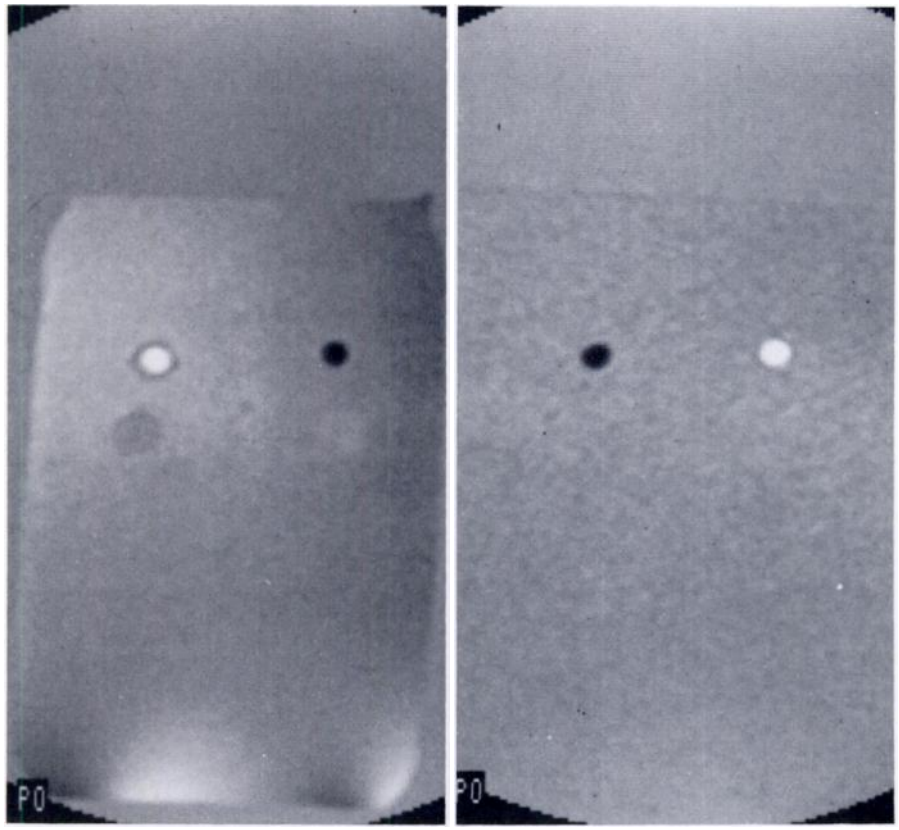

a. b.

Phase sensitive reconstruction of the negative sense velocity encoded data from the image in Figure 2a.
a. Reversed flow contrast and residual phase error artifacts.
b. Image data subtractions give a positive-minus-negative phase error compensated image.

Figure 5

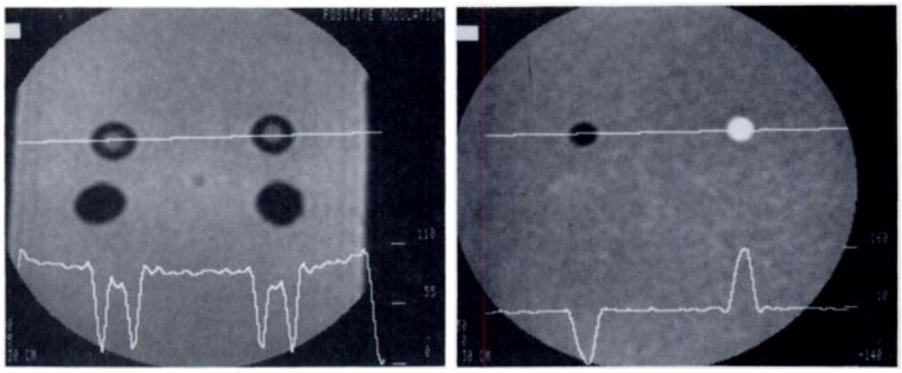

a. b.

Image value profiles are graphic overlays on the scans.

a. A density only phase insensitive reconstruction showing a differently windowed version of Figure 2b.

b. The true flow image of Figure 4b is shown in 2 × magnification.

posite sense scans to give an observed 160 units maximum, which is just twice (as discussed above) the single-scan conventional magnitude image of Figure 5a at the same location.

A simple fluid in non-rotational and non-turbulent flow, in a circular cross section tube, should give a parabolic velocity profile ideally, and the maximum velocity at tube-center is twice the average velocity. The central velocity corresponding to Figure 5b is, therefore, about 10 cm/sec. Using the numerical modulation factors for this scan given in Equation 2, the theory predicts a quarter cycle phase shift corresponding to a velocity of 10 cm/sec. The empirical result thus confirms this prediction within the experimental error of these trials.

In-the-plane Motion. Figure 6a shows a coronal scan, the section of which contains the upper flowing liquid U-tube, with conventional magnitude of magnetization reconstruction. We observe the semicircular bend projecting into air beyond the non-moving liquid container. Velocity sensitization is much larger here (see Equation 3) than for the transverse case discussed above, but for later reference we have maintained the flow velocity at the same 5 cm/sec average value used in Figures 3–5. Note the peculiar striated appearance of the flowing material even in the conventional reconstruction; these peculiarities disappear when the flow rate is reduced substantially. At an average velocity of 0.6 cm/sec the magnitude reconstruction shows a non-remarkable flowing liquid MR conventional image with image values at tube center of about 100 units.

The true flow image for in-the-plane velocity encoding is shown in Figure 6b, again using the positive-minus-negative modulation subtraction of image data to mitigate spurious phase artifacts. The non-moving liquid again largely vanishes into the zero-level background. Liquid flowing upward in the display images as negative values on the right of the viewed image, while liquid moving downward in the display images as positive values. The liquid moving around the top of the circle has ever decreasing vertical component of motion; it becomes less contrasting with background, therefore, and exhibits the predicted zero image values at the top of the tube where its velocity is perpendicular to the sensitized direction.

As explained previously for the case of transverse flow, the flow velocity was adjusted just below the level at which the central values of the flow image begin to decrease; this is approximately the one quarter cycle phase shift point, at which the measured average velocity was 0.6 cm/sec. Equation 3 predicts that the modulation parameters for this scan require a flow velocity of 1.3 cm/sec to attain quarter cycle shift. The maximum velocity for the observed 0.6 cm/sec average is 1.2 cm/sec, which we consider to agree with the 1.3 cm/sec prediction well within experimental error. We observe that the subtraction of two scans flow image gives flow profiles in Figure 6b rising to a maximum of about 200 units (positive and negative depending on the sense of flow) for a one quarter cycle phase modulation, which again confirms the prediction of being twice the 100 unit value observed in a single scan's conventional reconstruction.

Peripheral Results. If we compare the details of the true flow image at 0.6 cm/sec in Figure 6b with the conventional magnitude reconstruction image at much larger flow rates in Figure 6a, we find that the apparent width of the flowing liquid in the true flow image is greater than that in the magnitude reconstruction *i.e.*, the very fast flowing liquid image values are significantly *attenuated* in the conventional image, but this happens near the walls of the tube where the flow itself is small and the local change-of-flow rate is large. Near the tube center, where the velocity is itself largest the flowing-liquid remains bright.

This behavior confirms earlier suggestions that the attenuation of signal in conventional scans for flowing materials may largely be dominated by phase-shift blurring over the irresolution dimensions of the scanner (5). We speculate that this also is the origin for many of the scanner parameter dependent variations of flow effects observed by others in conventional scans of humans (5).

Recent interest also concerns differences in flow appearance for conventional MR images that occur in multi-echo imaging (21). Specifically,

Figure 6

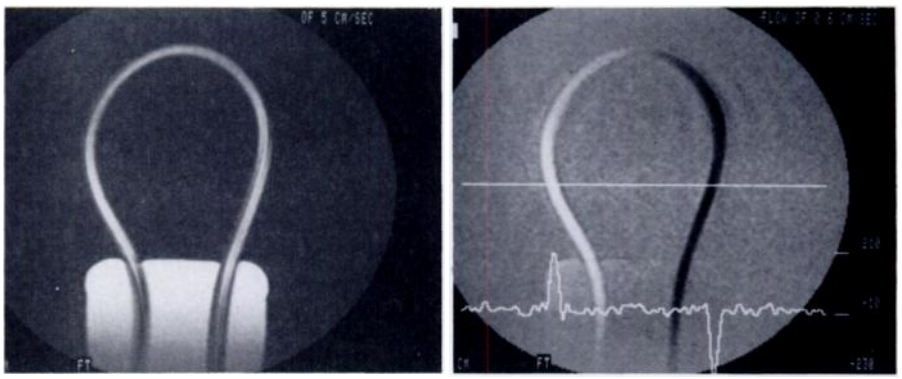

a. b.

a. A conventional magnitude reconstruction illustrates a coronal image through the phantom U-tube with average flow speed of 5 cm per second.

b. The phase reconstruction shows in-the-plane true flow imaging sensitized to vertical motion, at an average speed of 0.6 cm per second.

an important question is whether the data acquired in the second (or any even numbered) echo has completely rephased with respect to dephasing characterizing the first (or any odd numbered) echo. Our theoretical prediction for motion phase shifts, is that rephasing occurs only for gradients that are repeated successively between echoes, but that for a single modulation (such as we have discussed) successive rf echo pulses only invert the algebraic sign of the induced phase-modulation (8, 10). We applied the phase modulation technique also to a two echo Carr-Purcell transverse scan sequence and reconstructed the phase sensitive images for each echo. The first-echo image of Figure 7a appears identical with the second-echo image of Figure 7b, except for the predicted contrast inversion. We believe that second echo phase inversion in conventional MR scans cancels only the phase shift effects from the accidental modulations discussed above.[3] In particular, phase modulations arising from the selective 180° echo gradients and from the image readout gradients normally repeat the same way for both echoes.

This phase inversion effect of 180° rf pulses also explains why the contrast is inverted between the transverse and coronal scans in Figures 5 and 6. One is implemented by field gradient reversal modulation and the other by employing a 180° rf pulse between two positive sense pulses. In any event, these scans confirm the prediction that the requisite phase gradient bipolar modulation is equivalent (apart from the algebraic sign change) whether produced by gradient reversal or by rf echo pulse reversal.

Human Study Example. Figure 8 shows an extension of the cardiac gated true motion imaging to application in heart muscle velocity (8, 10). The transverse orientation scan has phase gradient modulation to sensitize the data to horizontal (as viewed) velocities. The modulation strength is just two thirds of that characterized by Equation 3, and we are purposefully exploiting the accidental modulation inserted into first echo data by readout gradients. Although cardiological interpretation is inappropriate here, the heart appears to be in early systole, and the dark linear outlines along the anterior and posterior walls in the conventional reconstruction of Figure 8a seem certainly to be severe velocity change artifacts. These outlines are not

Figure 7

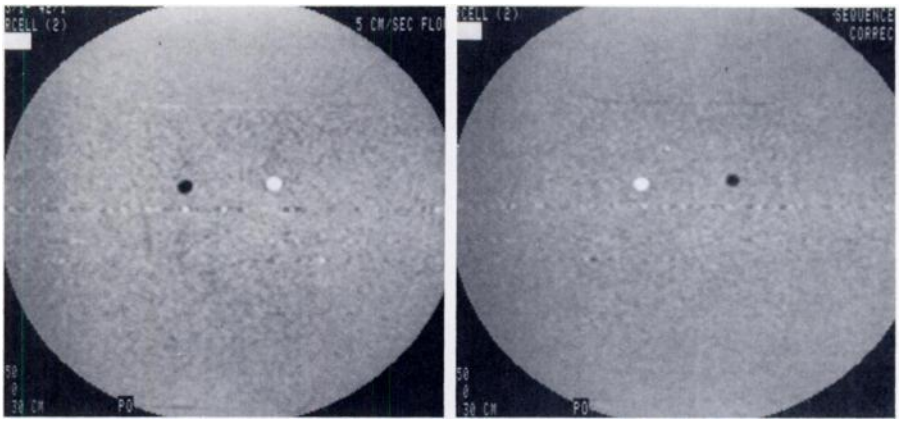

a. b.

a and b. True flow transverse images reconstructed from first and second echoes, respectively, of a multi-echo Carr-Purcell sequence. There is a single velocity encoding phase gradient modulation, and the second echo reconstruction displays a predicted phase contrast reversal.

evident in the phase-sensitive image of Figure 8b. We believe they originate from the same process as attenuates the conventional image MR values near the walls of the flow-tube in Figure 6a.

In the phase sensitive quadrature image reconstruction, shown in Figure 8b, positive contrast (brighter display) corresponds to motion toward the right (as viewed) while oppositely directed motion displays as negative contrast (blacker display). One can visualize horizontal motion imaging of structures with different speeds and in opposite directions quite readily in the scan, but the interpretation is uncontrolled in this crudely attempted trial. Motion to the right of sufficient speed to accumulate phase modulation, for example, of three quarter cycle will appear in the same contrast as slower leftward motion accumulating minus one quarter cycle, and so on. The technical name for this is *aliasing*, although we doubt it happens to occur in Figure 8b. Furthermore, severe phase error artifacts occur (at least as severe as the non-flowing phantom scan of Figure 3b) in the non-moving portions of the patient. We must suspect these phase artifacts contaminate the motion image generally.

We have not been able to apply the positive-minus-negative modulation image subtractions (described for fixed phantom scans) successfully to humans, as yet. The reasons involve a number of practical problems related to limitations imposed by our current software operating system. Moreover, we believe that the simplest phase sensitive reconstruction option, as well as the use of parent sequences not originally intended for true motion imaging, as used in these evaluation studies is far from the best choice for actual clinical application.

Figure 8

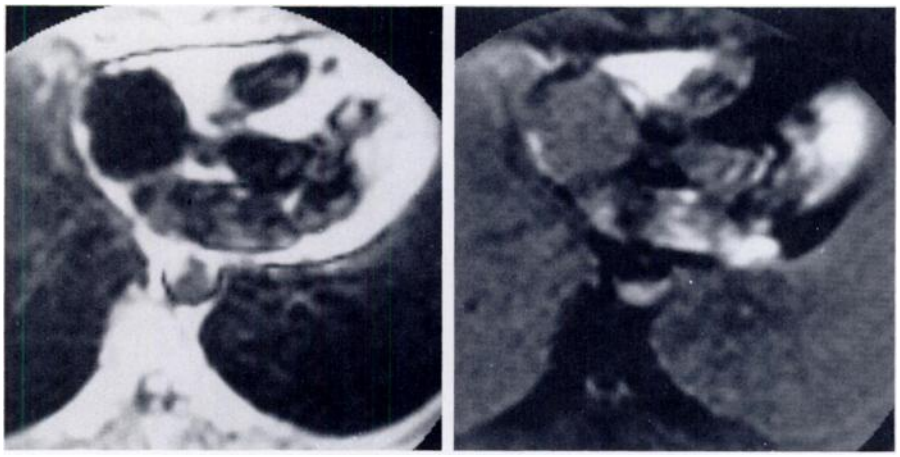

a. b.

a and b. A transverse image through the living human heart, obtained with cardiac gating, using optional reconstructions, respectively, for conventional density magnitude and for horizontal motion in-the-plane of the section.

[3] This cancellation of the readout-gradient *accidental* velocity-sensitizations will be, of course, of great practical importance in adapting the phase-gradient-modulation method to human clinical scan software.

Depending on the portion of anatomy scanned, attempts at sensitive phase modulation methods for blood flow imaging in humans have proved, without cardiac gating techniques, to be uncertain at best and completely obliterated by artifact at worst.

DISCUSSION

Confirmations. These evaluations, together with others mentioned in this paper, show extraordinary potential for many applications of the phase modulation method for true motion MR imaging. The experiments discussed here confirm and demonstrate all the essential theoretical predictions of the original proposal (8). These confirmations are both qualitative and quantitative:

- The bipolar phase gradient modulation can be interlaced into various normal MR scanning sequences (Figures 2 and 5–8). The resulting velocity-encoding does not depend upon T1 or T2 relaxation, nor upon selective excitation of some well-defined active volume.

- While standard phase insensitive reconstruction of the data yields a conventional image, various phase sensitive reconstruction options give a true motion MR image.

- Both the speed of motion and relative direction direction are revealed. In the simplified reconstruction, motion image values are given by the conventional image density multiplied everywhere by the trigonometric sine function of the velocity proportional phase shift of moving magnetization. This was demonstrated by the equal but opposite contrasts in Figures 4 and 5 for oppositely directed flows; the sinusoidal maximization at a one quarter cycle phase shift has a quantitative value agreeing with the predicted conventional-image water-values.

- Both non-moving magnetization and that moving perpendicular to the velocity-sensitizing direction give a true motion image of null-zero, *i.e.*, they show the same image contrast as the no-signal level from air (Fig. 5).

- All components of vector velocity may separately be selected for sensitization in true motion imaging. Transverse section scans in Figures 5 and 8 show, respectively, motion perpendicular to the image plane and motions horizontal in-the-plane, while the coronal scan example of Figure 6 demonstrates vertical motion sensitization in-the-plane.

- The velocity-sensitivity can be adjusted by controlling the bipolar modulation parameters according to the expression in Equation 1 (and velocity values thereby obtained without special flow calibration procedures). This is verified by excellent agreement between the empirical quantitative results and the prior theoretical predictions.

- Different specific implementations, *e.g.*, direct field gradient reversal in Figure 5 compared with rf echo pulse reversal of phase sense in Figure 6, give the same requisite velocity dependent phase gradient modulation.

- The flow profile traced in Figure 6 shows a signal-to-noise ratio of at least 20 at maximum velocity of 1.2 cm/sec. For unity signal-to-noise, the corresponding velocity would be 0.06 cm/sec; this supports the original estimate (8) of sensitivities of a few tenths millimeter/sec.

- In multi-echo sequences (see Fig. 7), even numbered echoes do not rephase the imposed single bipolar phase modulation of moving magnetization, but merely invert its algebraic sign.

- The velocity of molecules is the important quantity in MR motion imaging and not narrowly physical flow of fluids. Heart-wall motion in Figure 8b is imaged on the same physical basis as the water flow in a U-tube in Figure 6b.

- Conventional spin-echo sequences especially generate accidental bipolar phase gradient modulations. This sensitizes to velocity as readily as a purposefully added modulation. The heart scan in Figure 8 exploited this effect, but suggested that it was too uncontrolled for many clinical applications.

- A second (and complementary) phase sensitive image is the *real* (or the in-phase) reconstruction. It is less velocity sensitive than the quadrature reconstruction, behaves as the cosine function of the phase shift angle, and does not discriminate opposite directions of motion. Examples have been presented elsewhere (4, 5). These studies verify the predicted behavior because it is the root sum-of-squares of the sensitive quadrature image and the relatively insensitive in-phase image, which produce the conventional appearing magnitude reconstructions shown in this article.

- The velocity encoding phase modulations are special because of their unique temporal form and not because the field gradients required must be from separate physical coils than produce the conventional imaging gradient forms. One may, however, find true motion-imaging applications for which dedicated and specially designed modulation coils would provide significant advantages.

Limitations. Many limitations and cautions exist in applying the phase modulation method for motion-imaging (and they mostly apply to time-of-flight methods are well). First, conventional sequences can accidentally impose strong phase gradient modulations identical with those discussed in this article. Thus, a particular sequence may have hidden within it a velocity sensitization unappreciated by the operator. For example, in-the-plane motion of an artery during the heart cycle may dominate phase modulation and image reconstruction values, while the scanner user anticipates only sensitization to flow motion along the vessel. Sequences should carefully be studied and compensated for any such untoward modulations. Moreover, conventional reconstructions may reveal a variety of phase blurring artifacts, which might be mistaken for physical or physiological indications.

Current experience suggests that cardiac gating may be mandatory for any semblance of reliability in flow and motion MR imaging. Phase inconsistencies from view-to-view and erratic non-flow motions in the vicinity of large arteries are some of the problem causing effects in the absence of gating.

Phase error artifacts, unrelated to motion, in unmodulated scans occur in our system and have been admitted to exist in other systems (10–12) as well. These limit the ultimate sensitivity and reliability of true motion images by phase-modulation techniques. It appears necessary to *compensate* such artifacts (as well as any unavoidable and unwanted accidental modulations) by performing more than one level of bipolar phase gradient modulation in a motion-imaging scan. We have demonstrated a crude example by subtracting negative modulation data from positive modulation data (combined somtimes with no-flow modulation

data) in this article. While sufficient for demonstration purposes here, much more effective options exist, given appropriate software extensions.

Long-term patient displacement between separate scans is a most difficult problem in any scan subtraction procedure. Much better comparison and compensations are to be gained by acquiring differently modulated raw data chains on short term successive cycles and manipulating the raw data appropriately.

The large phase gradient modulation inherently produced by a conventional spin echo sequence, or by the selective 180°-rf-pulse used in multi-section scanning, is likely to prove the origin of undesired, substantial, and overwhelming motion dependent phase artifacts. A simple remedy in that case is to use the second (or any even numbered) echo of a multi-echo sequence, since the velocity term sensitized from accidental modulations cancels for even numbered Carr-Purcell echoes (we noted elsewhere [8], however, that a residual motion acceleration term remains).

Future Development. System spatial irresolution, or even subject intrinsic physical effects, guarantees some degree of motion phase blurring. A distribution of velocities, rather than a single velocity, exists in any spatially resolvable element. Unlike ordinary spatial blurring, which degrades only image sharpness, phase blurring can generate unacceptable image artifact. We demonstrated some examples in this study. Accidental velocity phase modulations, as well as phase errors unrelated to motion, correspond to some phase rotation, which varies unpredictably with velocity within the distribution. These are practical problems limiting the usefulness of the current crude approaches to true motion imaging. To some extent, the severity can be reduced by careful choice of the parent sequence parameters to minimize, from the beginning, strong accidental phase gradient modulations. Obvious similar observations apply to other systematic approaches, *e.g.*, the use of cardiac gating.

If several different and controlled motion encodings yield different data sets (also hopefully within a time interval minimizing patient movement), and if these are carefully chosen according to theoretical dictates, then one can resolve the velocity distributions into separate elements. In consequence, it turns out that phase errors characterizing each of those separate elements can readily be eliminated. When this occurs, then all the major limitations discussed in the preceding paragraph recede to much less bothersome levels. How much less bothersome will certainly depend upon how many different motion encodings occur, and this depends significantly on how much time is tolerable to complete a study. These studies demonstrate clearly, in Figures 3 and 4, that only two or three different phase gradient modulations produce remarkable improvements, even using current non-optimum methods.

An important advantage, in this regard, exists for motion imaging by the phase gradient modulation method. In practical scanners, it is common for conventional imaging to repeat each data cycle several times and average those data to improve system signal-to-noise ratios. We have shown here that conventional image information remains available, even after one introduces motion encoding pulses. What one does with the information is a post-scan, but pre-reconstruction option, if one saves all raw data in original form.

One option is to average magnitude reconstruction image data; one extracts high contrast detail, noise averaged conventional results, just as if conventional data cycle averaging had occurred. A second option is not precluded; one uses the differently motion encoded cycles to resolve instead the velocity distribution. These reconstructions then yield true motion images independently and free of phase error contamination. One saves the time penalty, by employing such a scheme, but loses some relative noise performance for the motion images. It is likely that motion images, however, may not require the exceptional contrast detail quality demanded of conventional anatomical structure MR images. Answers to the implied questions await further technical and clinical research.

In any event, these evaluation studies demonstrate quite clearly, we believe, emminently feasible applicability and a very exciting future for the phase gradient method of true motion MR imaging.

References

1. Singer JR. Blood flow rates by NMR measurements. Science 1959; 130:1652.
2. Battocletti JH, Halbach RE, Salles-Cunha SX, Sances A Jr. The NMR blood flowmeter—theory and history. Med Phys 1981; 8: 435–443, 445–451, 452–458.
3. Mills CM, Brant-Zawdazki M, et al. Nuclear magnetic resonance: principles of blood flow imaging. AJR 1984; 142:165–170.
4. Moran PR. Evaluation of phase-modulation method for NMR true flow imaging. Radiology 1983; 149 (P):206. Direct NMR imaging of internal motion in humans. Proceedings of the First Carolina Biomedical Engineering Conference, Triangle Park, North Carolina, 1984. North Carolina Biotechnology Center Publication, Research, Triangle Park, NC.
5. Moran PR, Moran RA. Imaging true motion velocity and higher order motion quantities by phase gradient modulation techniques in NMR scanners. In: Esser PD and Johnston RE, editors. Technology of Nuclear Magnetic Resonance. New York: Society for Nuclear Medicine, Inc., 1984:149–166.
6. Wendt RE III, Murphy PH, et al. Flow and motion in MRI: a tutorial introduction. In: Esser and Johnson, editors. Technology of Nuclear Magnetic Resonance. New York: Society for Nuclear Medicine, Inc., 1984: 121–136.
7. Singer JR, Crooks LE. NMR blood flow measurements in the human brain. Science 1983; 221:654–656.
8. Moran PR. A flow zeugmatographic interface for NMR imaging in humans. Mag Res Imaging 1982; 1:197–203.
9. Bryant DJ, Payne JA, Firmin DN, Longmore DB. Measurement of flow with NMR using a gradient pulse and phase difference technique. J Comput Asst Tomogr 1984; 8: 588–593.
10. van Dijk P. Direct cardiac NMR imaging of the heart wall and blood flow velocity. J Comput Asst Tomogr 1984; 8:429–436.
11. O'Donnell M. Multiple-echo blood flow using phase contrast MRI. Med Phys, submitted for publication.
12. O'Donnell M, Karr SG, Barber WD. Multiple-echo blood flow imaging using phase contrast (ab). Program of the Third Annual Meeting of the Society of Magnetic Resonance in Medicine, New York, August 13–17, 1984:561–562.
13. Smith LS, O'Donnell M, Karr SG, Leue WM. Cardiac gated flow measurement in NMR imaging (ab). Program of the Third Annual Meeting of the Society of Magnetic Resonance in Medicine, New York, August 13–17, 1984:690–691.
14. Feinberg DA, Crooks LE, et al. Fluid velocity vector components imaged by multi-spin-echo MRI (ab). Program of the Third Annual Meeting of the Society of Magnetic Resonance in Medicine, New York, August 13–17, 1984;229–230.
15. Norris G. Phase encoded NMR flow imaging (ab). Program of the Third Annual Meeting of the Society of Magnetic Resonance in Medicine, New York, August 13–17, 1984:559–560.
16. Wedeen V, Rosen B, Chesler D, Brady T. MR velocity imaging by phase display (ab). Program of the Third Annual Meeting of the Society of Magnetic Resonance in Medicine, New York, August 13–17, 1984:742–743.
17. Waterton J. A novel NMR . . . measurement of velocity flow distribution (ab). Program of the third Annual Meeting of the Society of Magnetic Resonance in Medicine, New York, August 13–17, 1984; 734–735.
18. Wendt RE III, Ford JJ, et al. NMR pulse sequence for rapid imaging of flow (ab). Program of the Third Annual Meeting of the Society of Magnetic Resonance in Medicine, New York, August 13–17, 1984:749–750.
19. Lent A. Technicare exhibit. Third Annual Meeting of the Society of Magnetic Resonance in Medicine, New York, August 13–17, 1984.
20. King KF, Moran PR. A unified description of NMR imaging, data-collection strategies, and reconstruction. Med Phys 1983; 11:1–14.
21. Waluch V, Bradley WG. NMR even echo rephasing in slow laminar flow. J Comput Asst Tomogr 1984; 8:594–598.

Paul R. Moran, Ph.D.
Department of Radiology
Bowman Gray School of Medicine
300 South Hawthorne Road
Winston Salem, North Carolina 27103